Hydrogen-Deficient Stars
ASP Conference Series, Vol. xxx, 2008
Werner & Rauch

Wolf-Rayet Analyses

Wolf-Rainer Hamann, Götz Gräfener, Achim Feldmeier, Lida Oskinova, Andreas Barniske, and Adriane Liermann

Universität Potsdam, Germany

Abstract. Wolf-Rayet (WR) stars are characterized by their emission-line spectra, which are formed in a fast and strong stellar wind. Adequate non-LTE model atmospheres are successfully applied for their spectral analysis.

The available models account for wind inhomogeneities ("clumping") in the approximation that clumps are optically thin. Recently we developed a statistical treatment for optically thick clumps. The porosity effect facilitates the emergence of X-rays in spite of strong continuum absorption. With porosity applied to line formation, strong spectral features become generally weaker, and the reported discrepancy between Hα and the P V resonance doublet in O star spectra can be reconciled without a further reduction of the mass-loss rate.

Mass-loss from hot stars is driven by radiation pressure. This has been worked out in hydrodynamical models for O stars, however on the expense of approximations in the radiative transfer. For WR stars such models used to fall short in explaining the high mechanical momentum of their strong winds. Only recently, we combined our Potsdam Wolf-Rayet (PoWR) code with the hydrodynamic equations and obtained self-consistent WR models, showing that the previous shortfalls were due to deficiencies in the radiative-transfer treatment.

The PoWR models were employed for analyzing a comprehensive sample of Galactic WN stars. The results show the separation of the WN stars in two distinct groups. The late-type WN stars (WNL) are very luminous, contain larger or smaller amounts of hydrogen in their atmosphere, and are probably hydrogen-burning stars which never crossed the HR diagram to the red side. The hydrogen-free early-type WN stars (WNE) are less luminous and stem from progenitors of lower initial mass after an excursion to the cooler part of the HRD. Hence most WNE stars have not evolved from WNL.

1. Introduction: Wolf-Rayet stars

Wolf-Rayet (WR) stars are characterized by their emission-line spectra, which are formed in a fast (order of 1000 km/s) and strong stellar wind. Spectra of the WN subclass are dominated by the lines of helium and nitrogen, while WC spectra are crowded by lines of carbon, oxygen and helium (see e.g. Fig. 1). WR stars are hydrogen-free or at least hydrogen-deficient. In contrast, O stars are hydrogen-rich, and their mass-loss rate is significantly lower, and only some of their spectral features originate from their wind.

The *standard model* for the expanding WR and O star atmospheres is based on the assumptions of spherical symmetry, stationarity, and large-scale homogeneity (cf. Sect. 2.). The velocity law $v(r)$ is usually adopted in form of the so-called β-law, i.e. the standard model is not hydrodynamically consistent. Free parameters are the mass-loss rate $\dot{M}$, terminal wind velocity v_∞, stellar lumi-

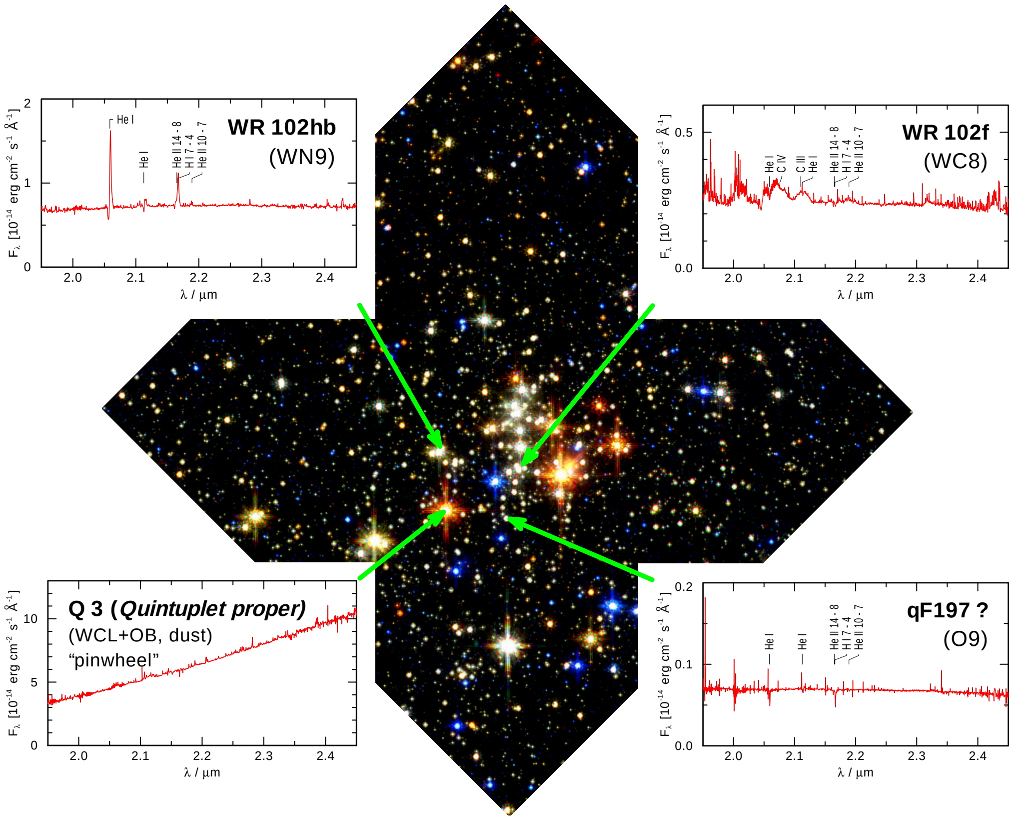

Figure 1. Examples of massive-star K-band spectra in the supermassive Quintuplet cluster in the Galactic center region (image:HST – PI D. Figer; spectra: ESO-VLT/SINFONI – Liermann, Oskinova & Hamann, in prep.)

nosity L_*, stellar temperature T_* (usually defined as the effective temperature related to the stellar radius R_* where the Rosseland optical depth reaches 10 or 20), and the chemical composition.

As WR emission lines are mainly formed in recombination cascades, the line flux scales with the square of the density. For "thin" WR winds, the continuum forms close to R_*. Approximately, this leads to an important parameter degeneracy: spectra simply scale with luminosity for models of the same T_* and the same "transformed radius" $R_\mathrm{t} \propto R_* \, \dot{M}^{-2/3}$. The normalized line spectrum thus depends only on two *spectroscopic parameters* (R_t, T_*) that are independent of the stellar distance, in analogy to $(T_\mathrm{eff}, \log g)$ for static stellar atmospheres.

In case of "thick" WR winds, in which even the continuum-forming layers are expanding with almost the terminal wind velocity, there is a further parameter degeneracy: the temperature T_* is automatically fixed for a given $\dot{M}$ and luminosity, and the normalized line spectrum depends solely on one parameter, $L/\dot{M}^{4/3}$. This case applies to most WC and a few WN stars.

The analysis of stellar-wind spectra requires adequate numerical simulations. Modeling such expanding atmospheres is a difficult task because of the extreme departures from local thermodynamical equilibrium (non-LTE), because

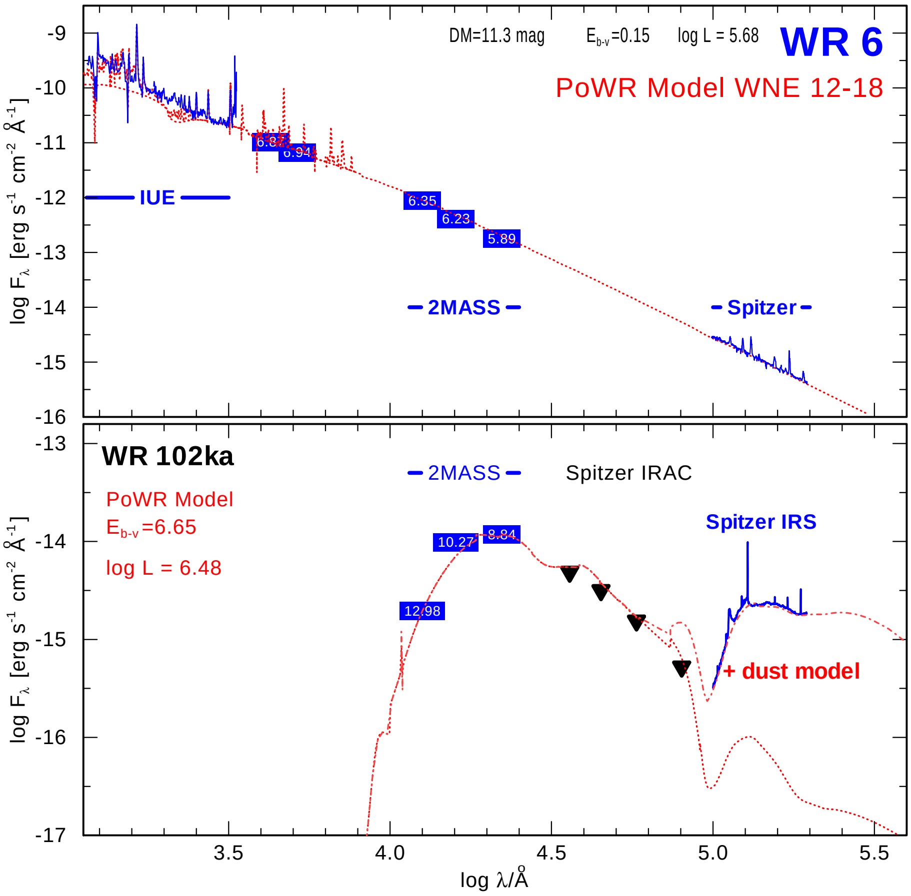

Figure 2. Spectral energy distributions from the UV to the mid-IR for two WN stars. For the WN4-type star WN 6 the observed SED (blue, noisy lines and photometry marks) is perfectly reproduced by the model (red/dotted line), including the mid-IR range recently observed with *Spitzer*. The observed SED of the WN10-type star WR 102ka, which is located in the Galactic center region and totally obscured in the UV and visual, shows an excess in the mid-IR that is not fitted by the stellar SED (red/dotted), but by a dust-emission model (red/dashed). After Barniske et al. (in prep.)

of the need to account for complex model atoms, especially for the iron-group elements with their millions of lines, and because of the supersonic expansion. Adequate codes have been developed and successfully applied e.g. by the Munich group (Puls, Pauldrach), Hillier (CMFGEN) and in Potsdam (PoWR).

Grids of PoWR models are available via a WEB interface[1]. The spectral energy distribution (SED) as well as detailed line spectra are provided for a wide range of parameters (so far only for WN stars). Examples for SED fits are shown in Fig. 2.

[1] `http://www.astro.physik.uni-potsdam.de/PoWR.html`

2. Clumped stellar winds

There is a variety of observational evidence that hot-star winds are in fact inhomogeneous, e.g. the time-variability of spectral features, the weakness of electron-scattering wings of strong WR emission lines (see below), or the very existence of X-ray emission (e.g. 14). Theoretically, time-dependent hydrodynamical models (3) predict the formation of strong shocks, caused by the "deshadowing" instability which occurs when radiation is intercepted by optically thick lines.

While earlier radiative-transfer calculations adopted a smooth, homogeneous stellar wind, a relatively simple first-order clumping correction was readily implemented into the model codes about one decade ago (cf. Hamann & Koesterke 1998, Hillier & Miller 1999). This is based on the approximation that all individual clumps are optically thin at all frequencies ("microclumping"). The clumps fill the fraction f_V of the volume (often taken constant over the whole wind), while the interclump space is assumed to be void. Hence the clump matter is denser by a factor $D = f_\mathrm{V}^{-1}$, compared with the homogeneous model of the same $\dot{M}$. As typical WR emission lines are formed in a recombination cascade, these lines are approximately invariant when microclumping is compensated for by a corresponding reduction of the mass-loss rate with $\dot{M} \propto \sqrt{f_\mathrm{V}}$ (see Fig. 3). Electron-scattering line wings, however, depend linearly on the density and therefore become weaker with smaller mass-loss rate, irrespective of clump-

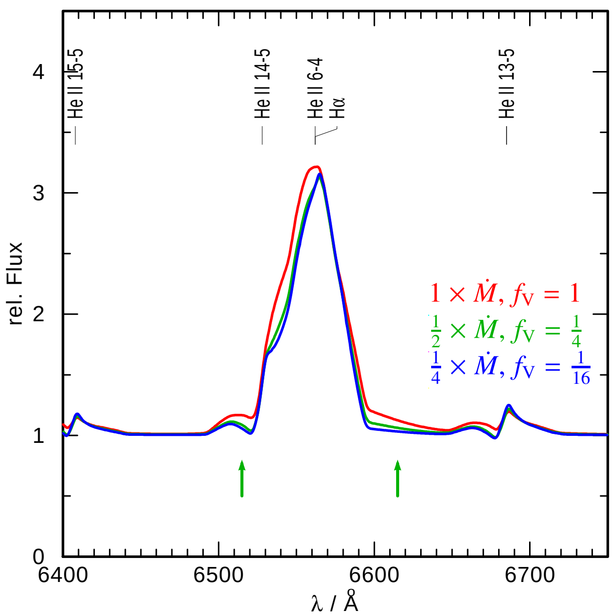

Figure 3. Model spectra for different filling factors f_V in the microclumping approximation. The effect of increased f_V is compensated by reducing the mass-loss rate by a factor of $\sqrt{f_\mathrm{V}}$. The emission-line spectrum remains nearly the same, except for the electron-scattering line wings (arrows) that are more pronounced for models with higher $\dot{M}$.

ing. Hence these wings provide a handle to estimate the degree of clumping. Resonance lines also depend linearly on ρ, but are practically of little diagnostic value because they are mostly saturated (see below).

However, the assumption of optically thin clumps is not generally justified, e.g. neither for strong lines nor for the continuum at X-ray frequencies. Recently we developed a more realistic treatment, which accounts for optically thick clumps ("macroclumping") in a statistical way. The effect of such clumping is a reduced *effective opacity*, because material that is shaded inside the clumps contributes less to the photon absorption.

X-rays from O stars, although commonly observed, should be absorbed by K-shell opacities before they can emerge from the stellar wind. One way to solve this discrepancy is to assume that the mass-loss rates are actually much smaller than obtained from UV/optical analyses with "standard" microclumping ($f_V = 0.1 \ldots 0.3$).

Alternatively, the emergence of X-rays can be facilitated by the porosity effect from macroclumping, as has been shown in analytical (4) and Monte-Carlo (13) modeling. Especially when the clumps are not spherical, but radially compressed, these models can nicely reproduce the shape of the observed X-ray line profiles.

Porosity is especially effective in spectral lines. Due to the Doppler effect, rays of a given observer's frame frequency can only interact with the corresponding surface of constant projected velocity. Macroclumping can be efficient in making this surface porous. Again using a statistical approach, we have implemented this effect in the formal integral of the PoWR code (15). First results for O and WR stars show that with realistic clump parameters all strong spectral features become significantly weaker.

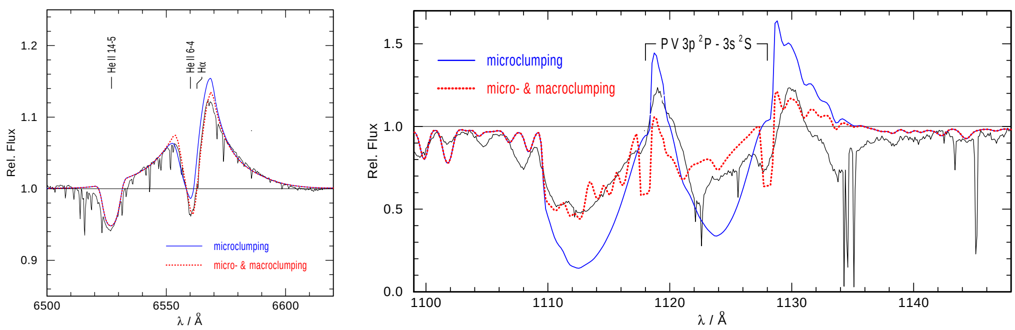

Figure 4. Effect of macroclumping on O-star spectra. The observed spectrum of ζ Pup is shown for comparison (black, ragged line). The model parameters correspond to ζ Pup. The solid (blue) line results from a model which only accounts for small-scale clumping with a density contrast $D = 10$. The dotted (red) curve is obtained with additional macroclumping in the formal integral. In case of the Hα emission (left panel) the effect of macroclumping is small. The right panel shows the region of the P V resonance doublet at 1118/1128 Å. (Numerous weak spectral features in this range are due to iron.) The usual modeling yields much too strong P Cygni features (blue, continuous line). With our macroclumping formalism, the line features are reduced to the observed strength (red, dotted curve).

In contrast to microclumping, the macroclumping affects not only the emission lines, but also the P Cygni profiles of resonance lines. In general, the prominent UV resonance doublets (C IV, N V, O VI) are saturated and therefore not sensitive to $\dot{M}$. The P V resonance line in the far-UV range observable with FUSE, however, is typically not saturated in O-star spectra, due to the small phosphorus abundance. This fact has been exploited recently by Fullerton, Massa, & Prinja (5) and Bouret et al. (1). As a very alarming result, they reported large discrepancies between the mass-loss rates derived from the Hα line and from the P V resonance doublet in O star spectra. One possible solution is by microclumping, when adopting a much larger clumping contrast and thus smaller mass-loss rates than believed hitherto. Such a reduction of O-star mass loss rates (by up to factor of 10!) would have far-reaching implications, e.g. for massive-star evolution, or stellar yields.

However, there is another possibility to explain these discrepancies, namely by optically thick clumping. The ρ^2 and ρ-linear diagnostics can be perfectly reconciled by accounting for macroclumping (see Fig. 4), thus avoiding to postulate smaller mass-loss rates.

Future research is needed in order to settle these questions, and thus to establish the true mass-loss rates from massive stars. Recently an international workshop was entirely devoted to *Clumping in Hot-Star Winds* (proceedings electronically published, cf. 10).

3. Hydrodynamical WR models

Mass-loss from O stars is driven by the momentum transfer from UV photons to the ions of heavy elements. This has been worked out in hydrodynamically self-consistent models for O stars, based on the fundamental concept of Castor, Abbott, & Klein (2). However, these "CAK models" fall short to explain the strong winds from WR stars. In fact, the rate of mechanical momentum in WR winds is often higher than achievable if each photon leaving the star transfers once its momentum $h\nu/c$ to the gas ("single-scattering limit").

Mass-loss exceeding this limit is possible in principle, but requires that photons deliver their momentum more than once. Such multiple-scattering effects are not properly included in the usual CAK-type models. Only recently, we combined the PoWR code with the hydrodynamic equations. The PoWR code treats the whole radiative transfer consistently, and thus automatically includes all possible multi-line effects. Indeed we obtain self-consistent WR models, as has been demonstrated in Gräfener & Hamann (7) for the WC5 prototype WR 111. Figure 5 demonstrates for this model how the inward and outward forces are perfectly balanced in the consistent, stationary hydrodynamic solution. Hence we are sure now that the winds of WR stars can be driven by radiation pressure. The previous shortfalls in explaining WR winds were obviously due to deficiencies in the conventional radiative-transfer treatment in CAK-type models.

Specifically in the dense winds from WR stars the multiple-scattering effects from the numerous lines of iron-group elements become important. But why the WR stars develop such a strong wind? According to our self-consistent HD models (see Fig. 6), the reason is their higher L/M ratio. WR stars are just close to the Eddington limit (where the radiation pressure on free electrons balances gravity, $\Gamma_e = 1$). Mass-loss rates of about $10^{-5} M_\odot$/yr, as typical for WR stars, are obtained for an Eddington Γ_e of 0.5 if the metallicity is solar. But even at very low metallicity, strong winds are predicted if Γ_e is sufficiently close to unity.

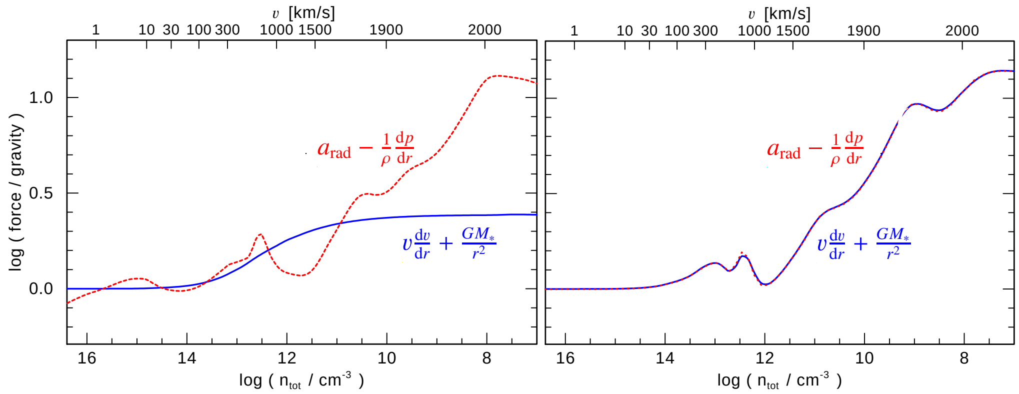

Figure 5. Acceleration as function of radius (represented by the atomic number density) for a WR atmosphere. In order to satisfy the hydrodynamic equation, the inward forces (inertia plus gravity, solid/blue line) must be balanced by the outward forces (radiative acceleration $a_{\rm rad}$ and pressure gradient, red/dotted curve). For a model with prescribed velocity field ("beta law") and mass-loss rate, the equality of both terms is not given (left panel). By incorporating the hydrodynamical equations into the PoWR model atmosphere code, a solution for $\dot{M}$ and $v(r)$ is found that is hydrodynamically consistent everywhere in the wind (right panel).

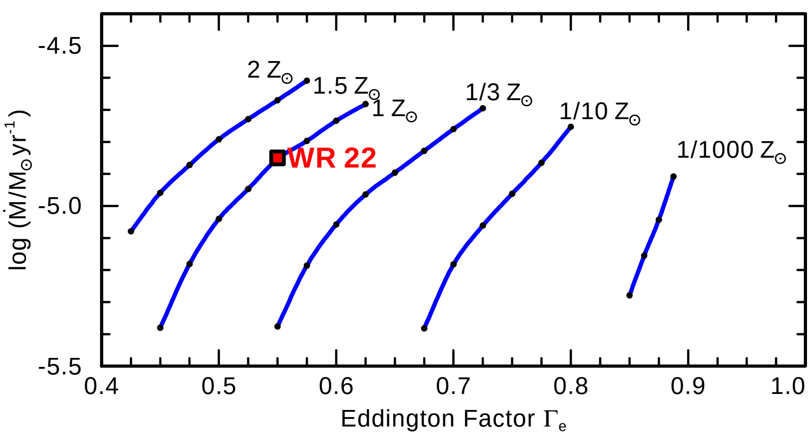

Figure 6. Mass-loss rates for models of the same luminosity ($10^{6.3} L_\odot$), but different L/M ratio (Eddington factor Γ) and different metallicities Z (compared to the solar metallicity $Z_\odot$). Hydrodynamically consistent PoWR models are represented by a black dot, blue lines connect models with the same metallicity. The empirical parameters of the WN7 star WR 22 are indicated by a red square. (From Gräfener et al., submitted)

4. The evolutionary status of WR stars

The condition for being close to the Eddington limit can be met by massive stars in two ways. This can be clearly seen from the empirical HRD in Fig. 7, obtained by Hamann, Gräfener, & Liermann (9) through analyzing a comprehensive sample of Galactic WN stars with the recent generation of PoWR models. The results reveal, more clearly than in previous work, the separation of the WN stars in two distinct groups. The WNL stars (WN stars with “late” subtype)

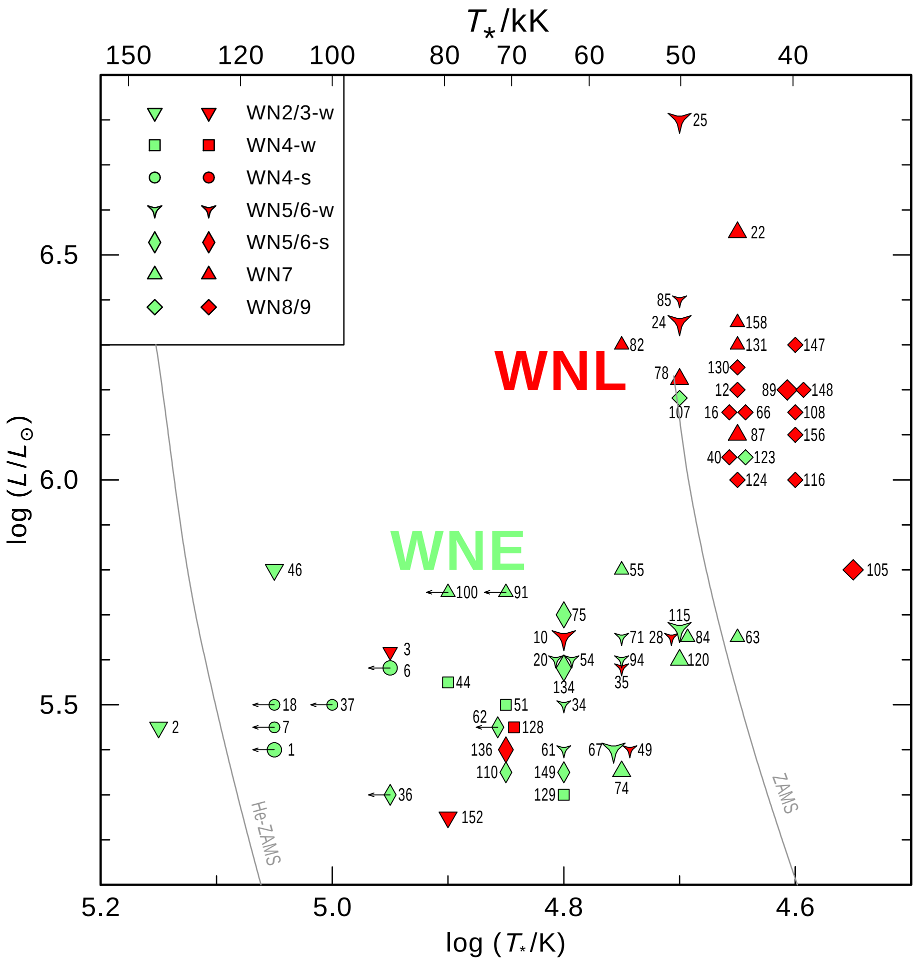

Figure 7. Empirical Hertzsprung-Russell diagram for Galactic WN stars. The labels denote the WR catalog numbers of the individual stars (some of them, like WR 22 and WR 25, are actually known as binary systems). The filling color of the symbols indicates the presence (red/dark) or absence (green/light) of atmospheric hydrogen. Small arrows indicate that T_* is only a lower limit. The slightly bigger symbols are for stars of known distance, i.e. more reliable L. The WN stars clearly split into two distinct groups divided by the hydrogen-ZAMS, the very luminous WNL stars with hydrogen and the less luminous, but hotter WNE stars without hydrogen.

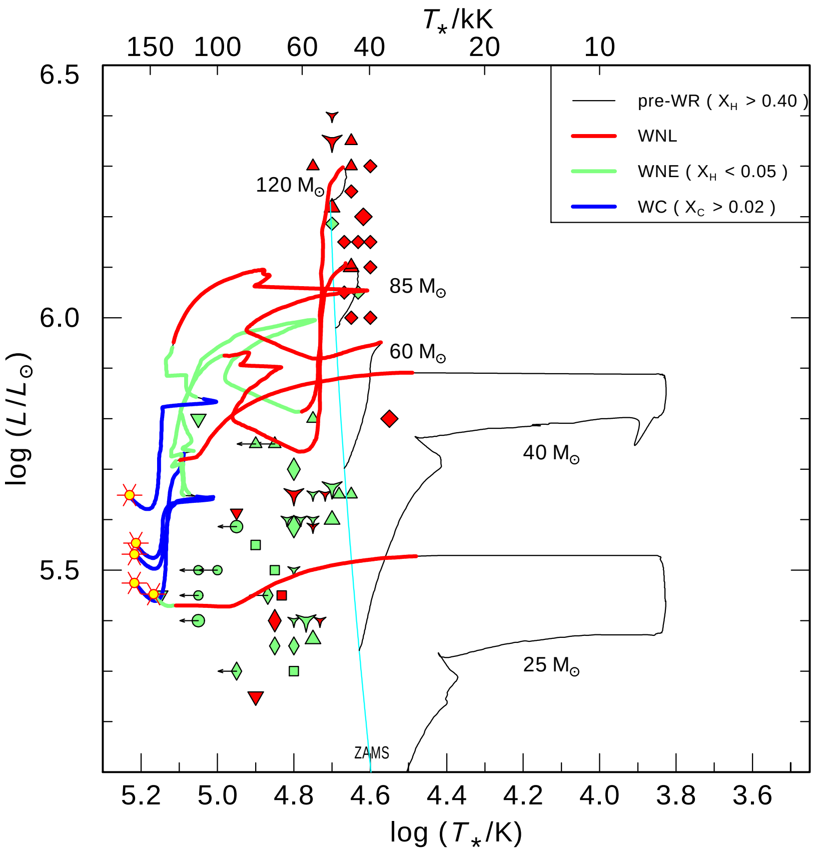

Figure 8. HRD with the analyzed Galactic WN stars, omitting known binaries. The symbols have the same meaning as in Fig. 7. The evolutionary tracks from Meynet & Maeder (12) account for the effects of rotation (labels: initial mass). The color/shading of the lines refers to the different evolutionary phases (see inset).

are very luminous, and contain more or less hydrogen in their atmosphere. They are close to the Eddington limit because of their paramount luminosities.

The WNE stars (WN of "early" subtype) are mostly free of hydrogen. They are less luminous than the WNL, but have higher temperatures placing them to the left from the hydrogen ZAMS. Thus they are helium burners, and for that reason have a high L/M ratio placing them close to the Eddington limit.

Evolutionary tracks for high-mass stars have been calculated by the Geneva group. In the version from Meynet & Maeder (12) these models account for the effects of rotation. In Fig. 8 we compare these tracks with our empirical WN parameters, now omitting the known close binaries which might have undergone mass exchange.

The comparison suggests that the WNL stars originate from the most massive progenitors of initially 60 ... 120 $M_\odot$. These stars spend all their life at the blue side of the HRD, and are still burning hydrogen in the center when appearing as WNL. Notably, the tracks with rotation do not show any excursions across the Humphreys-Davidson limit, in contrast to the tracks without rotation

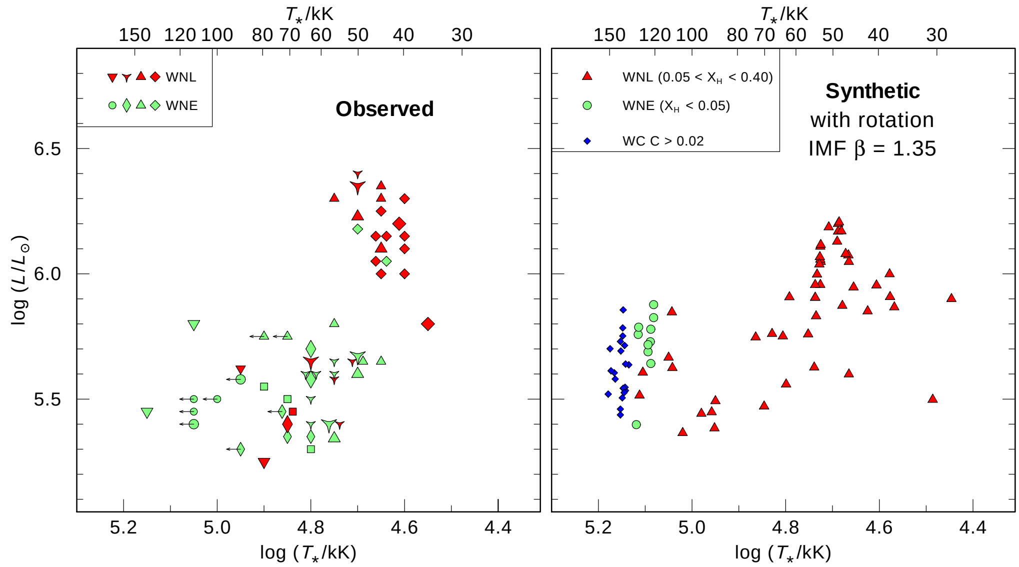

Figure 9. *Left panel:* HRD of the analyzed Galactic WN stars from Fig. 7, but without known close binaries. *Right panel:* Synthetic population, based on the Geneva tracks with rotation (cf. Fig. 8). The filling colors of the synthetic stars reflect their surface composition (dark/red: with hydrogen; light/green: almost hydrogen-free; blue/dark diamonds: WC-type).

which show such excursions. This may have implications for the interpretation of the LBV origin.

The HRD domain of the observed WNE stars is crossed by the evolutionary tracks for less than $\approx 40\,M_\odot$. The minimum initial mass for a star to reach the WR phase according to the Geneva models with rotation is $22\,M_\odot$. This is a clear advantage over the tracks without rotation, which predict SN explosions already in the red supergiant stage for all stars up to $37\,M_\odot$ initial mass. From their hydrogen-deficient atmosphere it is obvious that the WNE stars live from helium burning.

Hence the HRD in Fig. 8 suggests that WNL and WNE types do not form an evolutionary sequence. WNL and WNE stars rather originate from different ranges in initial mass.

However, comparing the empirical HRD just with tracks may be misleading, as lifetimes in different parts of the tracks are very different. Therefore we use the Geneva tracks to generate synthetic populations, which we can compare with the empirical HRD. We adopt the usual power law for the initial mass function (IMF) $dN = M^{-\beta-1}\,dM$ with exponent β=1.35 ("Salpeter IMF"). The star formation rate is set constant; this is only a rough approximation, as the analyzed sample contains several groups of stars that belong to the same association and are therefore probably coeval, which might not average out over the whole sample.

For the synthetic populations shown in Fig. 9 we created as many WN stars as our analyzed sample comprises (i.e. 59, without the proven close binaries). The result, shown in the right panel of Fig. 9, is disappointing when compared to the empirical HRD (left panel). Although the $25\,M_\odot$ track produces WN stars that are in the luminosity range observed for the WNE, these synthetic low-luminous WN stars are almost all of subtype WNL, showing high hydrogen abundances at their surface which would not escape detection.

Note that the observed sample contains more WNE than WNL stars. Taking the HRD positions, we find 39 WNE stars left of the ZAMS and 20 WNL stars on the right. On the basis of the hydrogen abundances, we have 33 WNE and 26 WNL. In contrast, the number of WNE (i.e. nearly hydrogen-free) stars in the synthetic sample is only 10. Hence the evolution predicts that less than one fifth of the WN stars are WNE, while more than half of the WN stars are actually observed to be hydrogen-free.

The stellar temperature of the WNE stars is another problem. In the evolutionary tracks the hydrogen-free surface appears only when the star has almost reached the helium main sequence. Observed WNE stars are mostly cooler, even when taking into account that some of the stars fall into the domain of parameter degeneracy. We conclude that many WNE stars have a larger photospheric radius than predicted by the stellar models. A speculative explanation is that there is a huge extended layer on top of the "real" hydrostatic core that expands only slowly (subsonic velocities), possibly driven by the "hot iron bump" in the mean opacity. "Strange mode pulsations" may be involved here, too.

The WNL group is also not reproduced well by the synthetic population, because their typical luminosity is smaller than observed. No synthetic star lies above $\log L/L_\odot = 6.2$, while the empirical HRD shows eight such stars of very high luminosity. Admittedly, only two of these stars have a known distance (WR 24 and WR 78), while the others rely on the subtype calibration. But even with this caveat, there seems to be a discrepancy.

Summarizing the comparison between the results of our spectral analyses of the Galactic WN stars and the predictions of the Geneva evolutionary calculations, we conclude that there is rough qualitative agreement. However, the quantitative discrepancies are still severe. It seems that the evolution of massive stars is still not satisfactorily understood.

References

Bouret, J.-C., Lanz, T., Hillier, D. J. 2005, A&A, 438, 301
Castor, J.I., Abbott, D.C., & Klein, R. 1975, ApJ, 195, 157
Feldmeier, A., Kudritzki, R. P., Palsa, R., Pauldrach, A. W. A., & Puls, J. 1997, A&A, 320, 899
Feldmeier, A., Oskinova, L. M., & Hamann, W.-R. 2003, A&A, 403, 217
Fullerton, A. W., Massa, D. L., & Prinja, R. K. 2006, ApJ, 637, 1025
Gräfener, G.,& Hamann, W.-R. 2005, A&A, 432, 633
Hamann, W.-R., & Koesterke, L. 1998, A&A, 335, 1003
Hamann, W.-R., Gräfener G., Liermann A. 2006, A&A, 457, 1015
Hamann, W.-R., Feldmeier, A., & Oskinova, L. 2007, Potsdam: Univ.-Verl., URN: http://nbn-resolving.de/urn:nbn:de:kobv:517-opus-13981
Hillier, D. J., & Miller, D. L. 1999, ApJ, 519, 354
Meynet, G., Maeder, A. 2003, A&A, 404, 975
Oskinova, L. M., Feldmeier, A., & Hamann, W.-R. 2004, A&A, 422, 675
Oskinova, L. M., Feldmeier, A., & Hamann, W.-R. 2006, MNRAS, 372, 313
Oskinova, L. M., Hamann, W.-R., & Feldmeier, A. 2007, A&A, (in press)